Acta Cryst F STRUCTURAL BIOLOGY COMMUNICATIONS

ISSN 2053-230X

Crystal structure of the starch-binding domain of glucoamylase from *Aspergillus niger*

Yousuke Suyama,[a] Norifumi Muraki,[b]‡ Masami Kusunoki[c] and Hideo Miyake[a]*

[a]Graduate School of Bioresources, Mie University, 1577 Kurimamachiya-cho, Tsu, Mie 514-8507, Japan, [b]Faculty of Bioresources, Mie University, 1577 Kurimamachiya-cho, Tsu, Mie 514-8507, Japan, and [c]Faculty of Life and Environmental Sciences, University of Yamanashi, 4-3-37 Takeda, Kofu, Yamanashi 400-8510, Japan. *Correspondence e-mail: miyake@bio.mie-u.ac.jp

Received 14 March 2017
Accepted 9 September 2017

Edited by A. Nakagawa, Osaka University, Japan

‡ Current affiliation: Institute for Molecular Science and Okazaki Institute for Integrative Bioscience, National Institutes of Natural Sciences, 5-1 Higashiyama, Myodaiji, Okazaki 444-8787, Japan.

Keywords: starch-binding domain; glucoamylase; β-sheet structure; disulfide bond; *Aspergillus niger*.

PDB reference: starch-binding domain of glucoamylase, 5ghl

Supporting information: this article has supporting information at journals.iucr.org/f

Glucoamylases are widely used commercially to produce glucose syrup from starch. The starch-binding domain (SBD) of glucoamylase from *Aspergillus niger* is a small globular protein containing a disulfide bond. The structure of *A. niger* SBD has been determined by NMR, but the conformation surrounding the disulfide bond was unclear. Therefore, X-ray crystal structural analysis was used to attempt to clarify the conformation of this region. The SBD was purified from an *Escherichia coli*-based expression system and crystallized at 293 K. The initial phase was determined by the molecular-replacement method, and the asymmetric unit of the crystal contained four protomers, two of which were related by a noncrystallographic twofold axis. Finally, the structure was solved at 2.0 Å resolution. The SBD consisted of seven β-strands and eight loops, and the conformation surrounding the disulfide bond was determined from a clear electron-density map. Comparison of X-ray- and NMR-determined structures of the free SBD showed no significant difference in the conformation of each β-strand, but the conformations of the loops containing the disulfide bond and the L5 loop were different. In particular, the difference in the position of the C^{α} atom of Cys509 between the X-ray- and NMR-determined structures was 13.3 Å. In addition, the *B* factors of the amino-acid residues surrounding the disulfide bond are higher than those of other residues. Therefore, the conformation surrounding the disulfide bond is suggested to be highly flexible.

1. Introduction

Glucoamylase (α-1,4-D-glucan glucohydrolase; EC 3.2.1.3) hydrolyzes the α-1,4- and α-1,6-glucosidic linkages of α-1,4-D-glucans such as starch, thereby liberating β-D-glucose (Koshland, 1953; Pazur & Ando, 1960; Hiromi, Hamauzu *et al.*, 1966; Hiromi, Takahashi *et al.*, 1966; Fierobe *et al.*, 1998). Glucoamylases are widely used commercially, for example in the production of glucose syrup from starch. The glucoamylases from *Aspergillus niger*, *A. awamori* and *Rhizopus oryzae* are especially important for industrial applications (Reilly, 1999; Pandey *et al.*, 2000; Pedersen *et al.*, 2000; Norouzian *et al.*, 2006). These glucoamylases contain a starch-binding domain (SBD) in the full-length protein that binds to starch and enhances the amylolytic rate (Hayashida *et al.*, 1989; Southall *et al.*, 1999; Rodríguez-Sanoja *et al.*, 2005). Three-dimensional structures of two glucoamylase SBDs have been analyzed. The first is from *R. oryzae*, belongs to carbohydrate-binding module (CBM) family 21 and its three-dimensional structure has been determined by NMR and X-ray crystallography, whereas the other is from *A. niger*, belongs to CBM family 20 and its three-dimensional structure has been determined by NMR (Liu *et al.*, 2007; Tung *et al.*, 2008). In both SBDs, two

Table 1
Crystallization information.

Method	Hanging-drop vapour diffusion
Plate type	24-well plates
Temperature (K)	293
Protein concentration (mg ml^{-1})	10
Buffer composition of protein solution	20 m*M* phosphate buffer pH 7.0
Composition of reservoir solution	2.0–2.3 *M* ammonium sulfate, 1.7%(*w*/*v*) PEG 400, 15%(*v*/*v*) glycerol, 85 m*M* HEPES pH 7.5
Volume and ratio of drop	4 µl (1:1 protein:reservoir solution)
Volume of reservoir (ml)	0.45

starch-binding sites were observed by structural analysis using bound β-cyclodextrin (β-CD), a cyclic starch analogue.

The full-length *A. niger* glucoamylase contains a catalytic domain and a C-terminal SBD. Thermal unfolding of both domains was observed by adiabatic differential scanning calorimetry (DSC; Tanaka *et al.*, 1995). Unfolding of the catalytic domain is irreversible, whereas that of the SBD is reversible. A disulfide bond is formed in the SBD between Cys509 and Cys604 (Sorimachi *et al.*, 1996). To elucidate the role of this disulfide bond in the SBD, we produced the wild type and several mutants lacking the disulfide bond, and thermodynamic studies were carried out (Tanaka *et al.*, 1998; Sugimoto *et al.*, 2007, 2009). The mutants are stabilized in terms of enthalpy, but a larger change in entropy overwhelms the enthalpic effect, resulting in destabilization. The three-dimensional structure of the glucoamylase SBD from *A. niger* was obtained by NMR, although the conformations of residues 509–512 and 601–606, which surround the disulfide bond, were unclear owing to a lack of nuclear Overhauser enhancement (NOE) constraints (Sorimachi *et al.*, 1996). Therefore, the aim of this study was to reveal the detailed conformation surrounding the disulfide bond of the *A. niger* SBD by X-ray crystal structural analysis.

2. Materials and methods

2.1. Crystallization

The purification of an SBD-containing fragment of the wild-type glucoamylase from *A. niger* was performed as described previously (Tanaka *et al.*, 1998). The purified protein was concentrated to 10 mg ml^{-1} and set up for crystallization at 293 K. The final optimized crystals were obtained from hanging-drop conditions using 2.0–2.3 *M* ammonium sulfate, 1.7%(*w*/*v*) PEG 400, 15%(*v*/*v*) glycerol, 85 m*M* HEPES pH 7.5 as the reservoir solution. The crystals grew to maximum dimensions of 0.3 × 0.4 × 0.3 mm in two weeks. For data collection, the crystals were flash-cooled in liquid nitrogen. Crystallization information is given in Table 1.

2.2. Data collection and processing

Multiple crystals were screened to identify a crystal with reasonable diffraction. The best data set was collected to 2.0 Å resolution under gaseous nitrogen (100 K) on beamline AR-NW12A at the Photon Factory, Tsukuba, Japan using X-rays at a wavelength of 0.978 Å. Data sets were processed and scaled using *HKL*-2000 (Otwinowski & Minor, 1997). Data-collection and processing information is shown in Table 2.

Table 2
Data-collection and processing information.

Values in parentheses are for the outer shell.

Diffraction source	Beamline AR-NW12A, Photon Factory
Wavelength (Å)	0.978
Temperature (K)	100
Detector	ADSC Quantum 210 CCD
Crystal-to-detector distance (mm)	150
Rotation range per image (°)	1
Total rotation range (°)	200
Exposure time per image (s)	1
Space group	*P*4
a, *b*, *c* (Å)	75.36, 75.36, 91.01
α, β, γ (°)	90, 90, 90
Mosaicity (°)	0.18–0.29
Resolution range (Å)	50.00–2.00 (2.03–2.00)
Total No. of reflections	291560
No. of unique reflections	34452 (1710)
Completeness (%)	99.9 (100)
Multiplicity	8.5 (8.2)
$\langle I/\sigma(I)\rangle$	79.8 (41.7)
$R_{\rm merge}$†	0.107 (0.164)
Overall *B* factor from Wilson plot (Å^2)	20.6

† $R_{\rm merge} = \sum_{hkl}\sum_i |I_i(hkl) - \langle I(hkl)\rangle| / \sum_{hkl}\sum_i I_i(hkl)$, where $I_i(hkl)$ is the *i*th measurement and $I(hkl)$ is the weighted mean of all measurements of I (hkl).

Table 3
Structure-solution and refinement information.

Values in parentheses are for the outer shell.

Resolution range (Å)	45.98–2.00 (2.052–2.000)
Completeness (%)	99.9
No. of reflections, working set	32650 (2401)
No. of reflections, test set	1734 (106)
Final $R_{\rm cryst}$	0.178 (0.200)
Final $R_{\rm free}$	0.229 (0.274)
No. of non-H atoms	
Protein	3351
Ion	20
Ligand	24
Solvent	204
Total	3599
R.m.s. deviations	
Bonds (Å)	0.021
Angles (°)	2.157
Average *B* factors (Å^2)	
Protein	26.35
Ion	46.30
Ligand	54.59
Water	33.81
Ramachandran statistics† (%)	
Favoured	96.46
Allowed	2.12
Outliers	1.42

† As determined by *MolProbity* (Chen *et al.*, 2010).

2.3. Structure solution and refinement

A molecular-replacement search using the program *BALBES* (Long *et al.*, 2008) and the FASTA sequence of SBD was performed to obtain the initial phases. Model building was performed using *Coot* (Emsley & Cowtan, 2004) in iterative

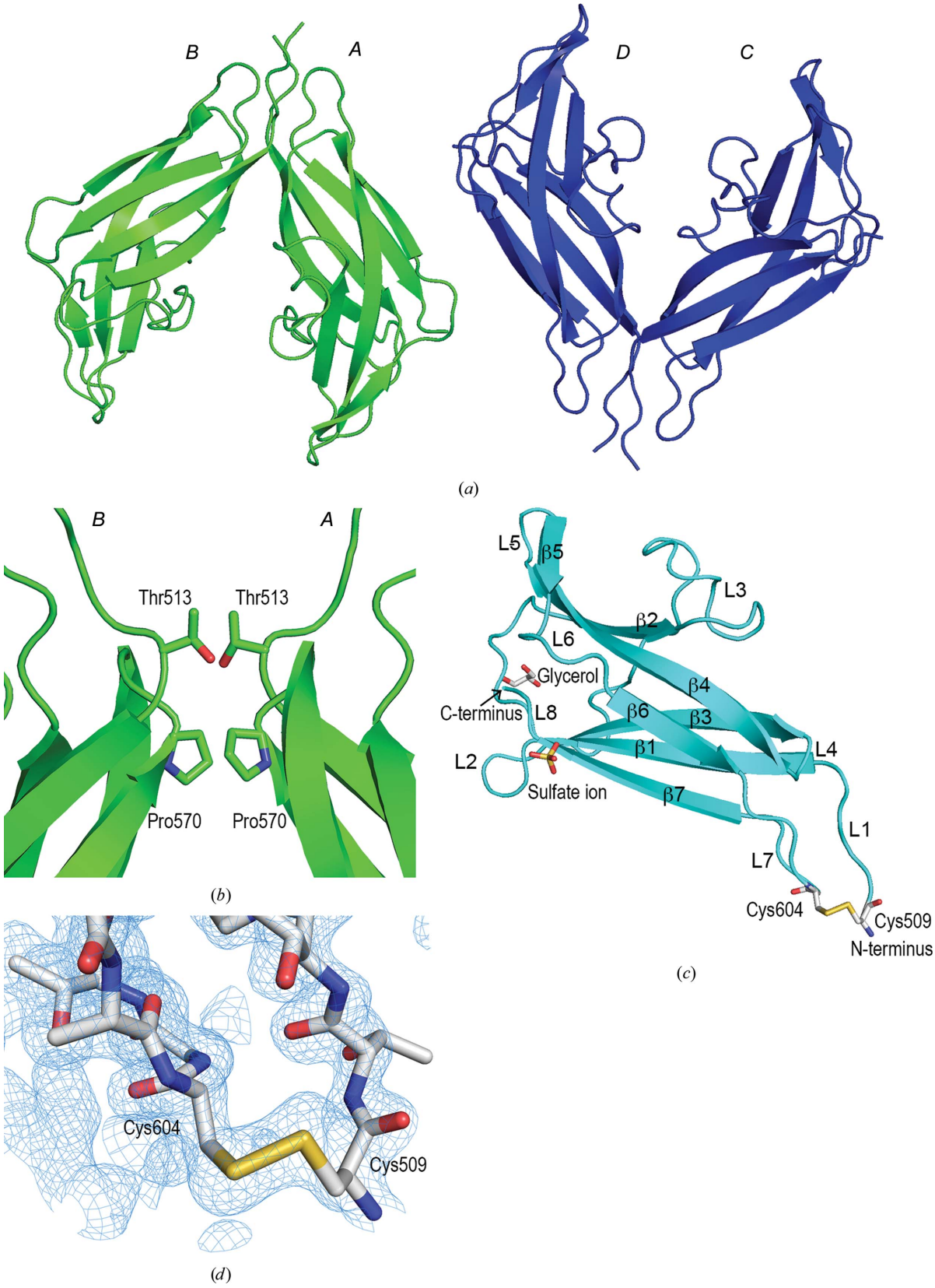

Figure 1
Crystal structure of the SBD (PDB entry 5ghl). (*a*) The asymmetric unit of the SBD is composed of four protein molecules, labelled *A*–*D*, which form two dimers (green and blue). (*b*) Interactions between the protein molecules. Thr513 and Pro570 in molecules *A* and *C* form hydrophobic interactions with the corresponding residues in molecules *B* and *D*, respectively. (*c*) Ribbon representation of the SBD, which consists of seven β-strands (β1–β7) and eight loops (L1–L8). A disulfide bond, a glycerol molecule and a sulfate ion are shown in stick representation. (*d*) Electron-density map surrounding the disulfide bond. The weighted $2F_o - F_c$ map (blue) is contoured at 1σ.

cycles with refinement using *REFMAC*5 (Murshudov *et al.*, 2011). Details of the structure solution and model refinement are shown in Table 3. Figures were prepared using *PyMOL* (v.1.7; Schrödinger).

3. Results and discussion

3.1. Overall structure

The SBD-containing polypeptide (amino acids 509–616) of *A. niger* glucoamylase was purified from an *Escherichia coli*-based expression system (Tanaka *et al.*, 1998) and the purified protein was crystallized at 293 K. The NMR structures of the SBD of *A. niger* glucoamylase (PDB entries 1kum, 1kul, 1aco and 1acz; Sorimachi *et al.*, 1996, 1997) were used as search models for molecular replacement in *CCP*4 (Winn *et al.*, 2011) but no phases were derived. A molecular-replacement search using *BALBES* (Long *et al.*, 2008) and the FASTA sequence of SBD was then completed, yielding a clear solution with one tetramer in the asymmetric unit. Finally, the structure was solved at 2.0 Å resolution. Four SBD molecules were observed in the asymmetric unit (Fig. 1*a*). The SBD exists as a monomer in solution, but forms a dimer with adjacent molecules in the crystal, two of which are related by a noncrystallographic twofold axis. Thr513 in molecules *A* and *C* forms hydrophobic interactions with the corresponding residues in molecules *B* and *D*, respectively (Fig. 1*b*). In a similar manner, Pro570 in molecules *A* and *C* forms hydrophobic interactions with the corresponding residues in molecules *B* and *D*, respectively (Fig. 1*b*). These interactions are considered to be caused by crystal packing. No interactions between the molecules were observed elsewhere. The SBD may have assumed a dimeric structure for crystal packing. The root-mean-square deviation (r.m.s.d.) of each molecule was 0.114–0.119 Å. The four SBD molecules showed almost the same structure in the crystal. The SBD was composed of seven β-strands and eight loops, with one glycerol molecule and one sulfate ion present per SBD molecule (Fig. 1*c*). These ligands are present in the reservoir solution and were therefore considered to be included in the crystal structure.

3.2. Conformation surrounding the disulfide bond

Cys509 and Cys604 are at the N- and C-termini, respectively, and they are linked by a disulfide bond (Sorimachi *et al.*, 1996). The presence of the disulfide bond was detected by NMR, but the conformation surrounding the disulfide bonds was unclear because the ^{15}N resonances were too broad (Sorimachi *et al.*, 1996, 1997). In this study, the X-ray crystal structure analysis showed electron density corresponding to a disulfide bond between Cys509 and Cys604, and the surrounding structure was revealed (Fig. 1*d*). The average *B* factor of all amino-acid residues of the SBD was 26.35 Å^2, but the *B* factor of the loop between residues Cys509 and Thr602 was as high as 44.22 Å^2. Together with the NMR-determined SBD structure, these results suggest that the conformation surrounding the disulfide bond is highly flexible.

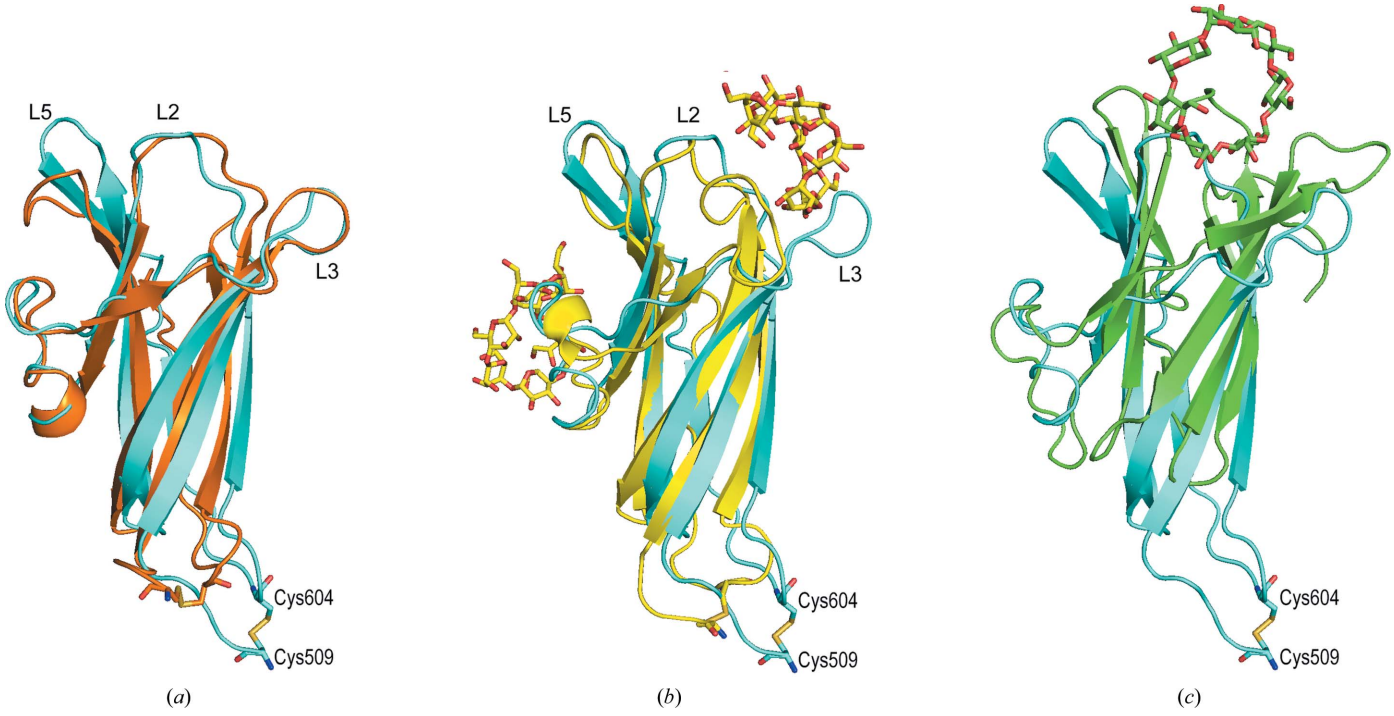

Figure 2
Overlay of the *A. niger* free SBD structure determined by X-ray diffraction (cyan) with (*a*) the *A. niger* free SBD structure determined by NMR (orange; PDB entry 1kum), (*b*) the *A. niger* SBD–β-CD complex structure determined by NMR (yellow; PDB entry 1ac0) and (*c*) the *R. oryzae* SBD–β-CD complex structure determined by X-ray diffraction (green; PDB entry 2v8l). The NMR-determined structures of SBD used were minimized average structures.

3.3. Comparison of X-ray and NMR structures of the SBD

The X-ray and NMR structures (PDB entry 1kum) of free *A. niger* glucoamylase SBD were compared, and the r.m.s.d. was 1.91 Å. No significant difference in the conformation of each β-strand was found, but the conformations of the loops (L1 and L7) containing the disulfide bond and the L5 loop were different (Fig. 2*a*). In particular, the difference in the position of the C^{α} atom of Cys509 between the X-ray and NMR structures was 13.3 Å. In contrast, in comparison with the NMR-determined structure of the SBD–β-CD complex (PDB entry 1ac0) the r.m.s.d. was 2.9 Å, and the conformational change of the L5 loop was smaller than that of the free SBD structure determined by NMR. However, the L3 loop flipped by about 90°, and the difference in position of the C^{α} atom of Ser559 in the L3 loop between the free X-ray structure and the NMR-determined structure of the SBD–β-CD complex was 15.5 Å (Fig. 2*b*). In both X-ray- and NMR-determined structures of free SBD, the L3 loop showed the same conformation, and thus binding of β-CD to the SBD seems to flip the loop largely owing to interaction with β-CD.

3.4. Comparison with the glucoamylase SBD from *R. oryzae*

The three-dimensional structure of only the SBD from *R. oryzae* glucoamylase has been determined (Liu *et al.*, 2007; Tung *et al.*, 2008). Therefore, we compared the *A. niger* free SBD structure determined by X-ray diffraction and that of the SBD from *R. oryzae* complexed with β-CD (PDB entry 2v8l; Tung *et al.*, 2008; Fig. 2*c*). The r.m.s.d. was 5.89 Å owing to the *A. niger* SBD being composed of seven β-strands and the *R. oryzae* SBD of nine β-strands. In addition, β-strands β2 and β3 in *A. niger* SBD were parallel, whereas all of the β-strands in the *R. oryzae* SBD were antiparallel. Furthermore, the structures surrounding the N- and C-termini were quite different in the two SBDs. Most glucoamylases are composed of a catalytic domain and an SBD; the SBD of *A. niger* glucoamylase is located at the C-terminus, whereas that of *R. oryzae* is located at the N-terminus. This difference in the position of the SBD relative to the catalytic domain probably caused the difference in structure near the N- and C-termini. Thus, the position of the β-CD-binding site was probably also different.

In our previous study, thermodynamic analysis of the *A. niger* SBD and its disulfide-bond-deficient mutants showed that the disulfide bond plays an important thermodynamic role in the stability of the protein. In this study, the conformation surrounding the disulfide bond of *A. niger* SBD was clarified using X-ray crystal structural analysis. In the future, structural analysis of disulfide-bond-deficient mutants will allow determination of the stabilizing effects of the disulfide bonds in glucoamylase SBDs.

Acknowledgements

The authors are very grateful to Professor Akiyoshi Tanaka of Mie University for continued support of this study. This work was performed under the approval of the Photon Factory Program Advisory Committee (Proposal No. 2005G289).

References

Chen, V. B., Arendall, W. B., Headd, J. J., Keedy, D. A., Immormino, R. M., Kapral, G. J., Murray, L. W., Richardson, J. S. & Richardson, D. C. (2010). *Acta Cryst.* D**66**, 12–21.
Emsley, P. & Cowtan, K. (2004). *Acta Cryst.* D**60**, 2126–2132.
Fierobe, H. P., Clarke, A. J., Tull, D. & Svensson, B. (1998). *Biochemistry*, **37**, 3753–3759.
Hayashida, S., Nakahara, K., Kanlayakrit, W., Hara, T. & Teramoto, Y. (1989). *Agric. Biol. Chem.* **53**, 143–149.
Hiromi, K., Hamauzu, Z. I., Takahashi, K. & Ono, S. (1966). *J. Biochem.* **59**, 411–418.
Hiromi, K., Takahashi, K., Hamauzu, Z. I. & Ono, S. (1966). *J. Biochem.* **59**, 469–475.
Koshland, D. E. Jr (1953). *Biol. Rev.* **28**, 416–436.
Liu, Y.-N., Lai, Y.-T., Chou, W.-I., Chang, M. D.-T. & Lyu, P.-C. (2007). *Biochem. J.* **403**, 21–30.
Long, F., Vagin, A. A., Young, P. & Murshudov, G. N. (2008). *Acta Cryst.* D**64**, 125–132.
Murshudov, G. N., Skubák, P., Lebedev, A. A., Pannu, N. S., Steiner, R. A., Nicholls, R. A., Winn, M. D., Long, F. & Vagin, A. A. (2011). *Acta Cryst.* D**67**, 355–367.
Norouzian, D., Akbarzadeh, A., Scharer, J. M. & Moo Young, M. (2006). *Biotechnol. Adv.* **24**, 80–85.
Otwinowski, Z. & Minor, W. (1997). *Methods Enzymol.* **276**, 307–326.
Pandey, A., Nigam, P., Soccol, C. R., Soccol, V. T., Singh, D. & Mohan, R. (2000). *Biotechnol. Appl. Biochem.* **31**, 135–152.
Pazur, J. H. & Ando, T. (1960). *J. Biol. Chem.* **235**, 297–302.
Pedersen, H., Beyer, M. & Nielsen, J. (2000). *Appl. Microbiol. Biotechnol.* **53**, 272–277.
Reilly, P. J. (1999). *Starch/Stärke*, **51**, 269–274.
Rodríguez-Sanoja, R., Oviedo, N. & Sánchez, S. (2005). *Curr. Opin. Microbiol.* **8**, 260–267.
Sorimachi, K., Jacks, A. J., Le Gal-Coëffet, M. F., Williamson, G., Archer, D. B. & Williamson, M. P. (1996). *J. Mol. Biol.* **259**, 970–987.
Sorimachi, K., Le Gal-Coëffet, M. F., Williamson, G., Archer, D. B. & Williamson, M. P. (1997). *Structure*, **5**, 647–661.
Southall, S. M., Simpson, P. J., Gilbert, H. J., Williamson, G. & Williamson, M. P. (1999). *FEBS Lett.* **447**, 58–60.
Sugimoto, H., Nakaura, M., Kosuge, Y., Imai, K., Miyake, H., Karita, S. & Tanaka, A. (2007). *Biosci. Biotechnol. Biochem.* **71**, 1535–1541.
Sugimoto, H., Nakaura, M., Nishimura, S., Karita, S., Miyake, H. & Tanaka, A. (2009). *Protein Sci.* **18**, 1715–1723.
Tanaka, A., Fukada, H. & Takahashi, K. (1995). *J. Biochem.* **117**, 1024–1028.
Tanaka, A., Karita, S., Kosuge, Y., Senoo, K., Obata, H. & Kitamoto, N. (1998). *Biosci. Biotechnol. Biochem.* **62**, 2127–2132.
Tung, J.-Y., Chang, M. D.-T., Chou, W.-I., Liu, Y.-Y., Yeh, Y.-H., Chang, F.-Y., Lin, S.-C., Qiu, Z.-L. & Sun, Y.-J. (2008). *Biochem. J.* **416**, 27–36.
Winn, M. D. *et al.* (2011). *Acta Cryst.* D**67**, 235–242.